Commercial Fe- or Co-containing carbon nanotubes as catalysts for NH_3 decomposition†

Jian Zhang,[a] Massimiliano Comotti,[b] Ferdi Schüth,[b] Robert Schlögl[a] and Dang Sheng Su*[a]

Received (in Cambridge, UK) 23rd January 2007, Accepted 31st January 2007
First published as an Advance Article on the web 21st February 2007
DOI: 10.1039/b700969k

Fresh commercial carbon nanotubes (CNTs) containing residual Co or Fe nanoparticles are highly active for NH_3 decomposition while the microstructure of CNTs remains unchanged. The catalysts are promising for elimination of NH_3 from coal gasification stream and for production of H_2 from NH_3.

Liquid NH_3 is seen as a promising carrier for H_2 due to its unique advantages over other liquid fuels, *i.e.* well-established infrastructure, high gravimetric storage capacity (17 wt%), production of inherently CO_x-free H_2, *etc.*[1] Recently, renewed interest in this catalytic process has increased by the growing requirement of high-quality H_2 for fuel cells.[2,3] In addition, ammonia decomposition is an option to remove NH_3 from the product stream of coal gasification/partial oxidation. Traditional commercial catalysts for NH_3 decomposition are based on Fe or Ni. Although a number of highly active catalysts have been continuously reported, their high metal loading and complicated synthesis route are the major obstacles for commercialization.[3,4] Ru is the most active metal for this reaction. However, the large scale application of Ru-based catalysts seems to be prevented by the limited availability and high price of Ru.[5]

In this contribution we explore the application of commercial CNTs as catalyst for NH_3 decomposition. In these carbon nanotubes, transition metals resulting from the production process are present in a highly dispersed state and should thus be very active. Chemical vapour deposition (CVD) over metal-based solid catalysts has been used to produce CNTs on a large scale.[6,7] Fe,[8] Co,[9] and Ni[10] are typical active phases to catalyze growth of carbon nanotubes. During the synthesis process, metal nanoparticles always remain in the raw products. Great efforts have been continuously made to purify CNTs by using corrosive chemicals.[11] However, if the properties of the residual transition metal nanoparticles could be catalytically exploited, as-synthesized carbon nanotubes could be interesting materials for catalytic applications.

The as-synthesized CNTs were used as catalysts without any additional chemical pretreatment. The catalytic performance is comparable with or higher than that of a commercial catalyst for NH_3 decomposition. Our work reveals that commercial CNTs are highly active catalysts for NH_3 decomposition. While the temperatures still seem high to be used in connection with hydrogen generation for fuel cells, the metal normalized activities substantially exceed those of the commercial catalysts.

Two typical commercial CNTs, *i.e.* Co- and Fe-containing CNTs from Bayer Materials Science AG (Baytubes C150P) and Applied Sciences Inc. (PSLD-24), respectively, were tested. Elemental analysis revealed that the content of residual ashes in the Co- and Fe-containing CNTs are 4.1 and 2.8 wt%, respectively. 100 mg of sample (pellets, 200–400 μm) were loaded in a quartz tube fixed bed reactor for catalytic evaluation. Pure gaseous NH_3 was passed through the catalyst bed and the temperature was increased to 700 °C with a heating rate of 20 °C min^{-1}. The effluent gas was analyzed by an on-line gas chromatograph (3000A MicroGC, Agilent), equipped with two lines, a PLOTU pre-column/Molsieve column combination with Ar as carrier gas for N_2, H_2 and CH_4, and a PLOTU column with He as carrier gas for NH_3 and CH_4. Both lines were equipped with TCD detectors. Scanning electron microscopy (SEM) was performed in a Hitachi S4800 electron microscope with an EDAX Energy Dispersive X-ray (EDX) detector. The microstructure of both CNTs and metal particles were examined *ex-situ* in a Philips CM200 FEG transmission electron microscope (TEM) equipped with electron energy loss spectroscopy (EELS) and EDX detectors.

Typical SEM and TEM micrographs of the two commercial CNTs are shown in Fig. S1, ESI.† Metal particles could be clearly seen in back-scattered electron SEM images. TEM images revealed that many metal particles are exposed and supported on the walls of the CNTs. The presence of Fe and Co as the most abundant metal were proved by EDX technique (data for Co shown as example in Fig. S2, ESI†).

These residual metal particles are nano-sized and size distributions of Co- and Fe-containing nanoparticles are 4–20 and 10–50 nm, respectively. As shown in Fig. 1, the Co-containing

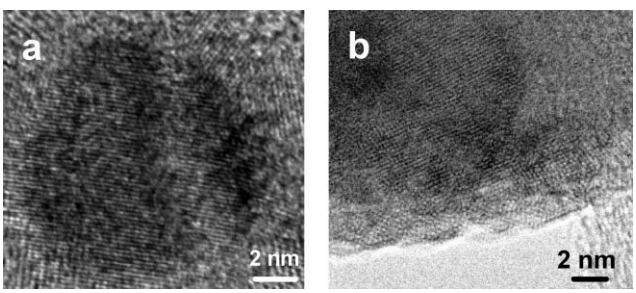

Fig. 1 HRTEM images of fresh (a) Co- and (b) Fe-containing particles in the tested CNTs.

[a]*Fritz Haber Institute of the Max Planck Society, Faradayweg 4-6, D-14195, Berlin, Germany. E-mail: dangsheng@fhi-berlin.mpg.de; Fax: +49 30 8413 4401; Tel: +49 30 8413 5406*
[b]*Max-Planck-Institut für Kohlenforschung, Kaiser-Wilhelm-Platz 1, D-45470, Mülheim a.d. Ruhr, Germany*

† Electronic supplementary information (ESI) available: SEM and TEM images (S1) and EDX spectra (S2) of the fresh CNTs and XPS spectra (S3) of the fresh and used CNTs. See DOI: 10.1039/b700969k

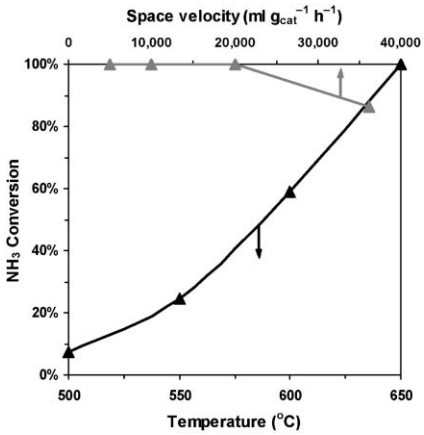

Fig. 2 Effects of reaction temperature and space velocity on NH_3 conversion over Co-containing CNTs. Black triangles: 100 mg catalyst, pure NH_3, 5000 ml g_{cat}^{-1} h^{-1}; gray triangles: 100 mg catalyst, 700 °C.

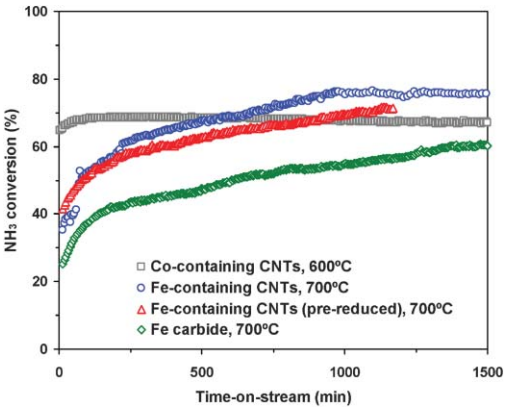

Fig. 3 Conversion as function of time for NH_3 decomposition over metal-containing CNTs and over iron carbide for comparison (50–100 mg catalyst, 5000 ml g_{cat}^{-1} h^{-1}).

nanoparticles are present as Co_2O_3 phase, while Fe-based nanoparticles consist of carbides and oxides.

The product gas leaving the reactor always contains exclusively N_2, H_2 and unreacted NH_3; no signals corresponding to CH_4 due to methanation of carbon could be detected by GC in any run. Fig. 2 reports NH_3 conversions over Co-containing CNTs under different reaction conditions. It can be seen that NH_3 conversion increases with increasing reaction temperature. An almost complete conversion of NH_3 could be achieved at 650 °C at a space velocity of 5000 ml g_{cat}^{-1} h^{-1}. When we fixed the temperature at 700 °C, even at a space velocity as high as 20000 ml g_{cat}^{-1} h^{-1}, NH_3 could be almost completely decomposed into N_2 and H_2. Further increase in space velocity to 36000 ml g_{cat}^{-1} h^{-1} resulted in a slight decrease in conversion, but the value was still as high as 86%. As shown in Fig. 3, the Co-containing CNTs showed a good stability in the reaction for 1500 min.

For Fe-containing CNTs, a remarkably long activation period of about 1200 min was observed, as shown in Fig. 3. During this period, NH_3 conversion gradually increased and approached a steady state at 76%. This could be due to several reasons, such as surface reconstruction, bulk reaction to other iron species, *etc*. Pre-reduction by H_2 did not change the general tendency, suggesting that the activation phenomenon is not caused by reduction of iron oxide. Fe carbide nanoparticles supported on activated carbon were also tested, and a similar activation period was observed. Considering the initial activity of each sample, we can conclude both, metallic Fe or Fe carbide, have some activity for this reaction, but are probably not the most active phase.

However, detailed analysis suggests that FeN_x is the primary active phase in Fe-containing CNTs, as is directly observed by HRTEM and EELS with elemental maps. As evidenced in Fig. 4, peaks assigned to N–K (401 eV), O–K (541 eV), Fe–L3 (711 eV) and Fe–L2 (723 eV), are present in EELS spectra. The particle consists mainly of Fe and N. The highly exposed part is N-rich while the N signal is weak on the boundary with CNTs. Trace amount of O might arise from possible oxidation after air exposure for TEM tests. Crystallographic analysis from the HRTEM images of used samples showed that the core of the particles is mainly iron carbide while the shell with a thickness of about ten atomic layers is the iron nitride phase. It seems plausible to

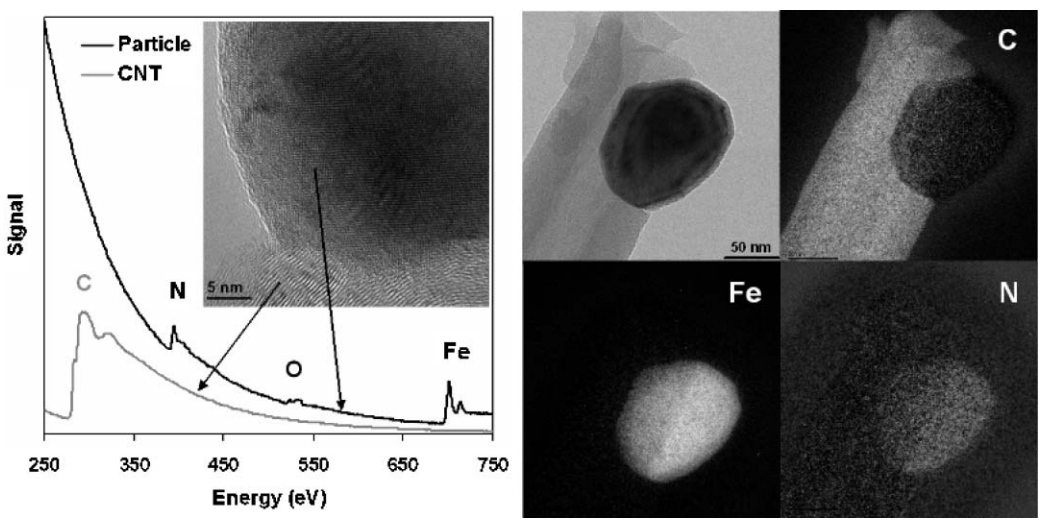

Fig. 4 HRTEM and EELS spectra (left) with element mapping images (right) of used Fe-containing CNTs.

Table 1 Catalytic activity of various catalysts for NH_3 decomposition

Catalyst	Metal content/wt%	T/°C	SV/h^{-1}	NH_3 conv. (%)
Co-containing CNTs	4.1% Co	700	20000	~100
Fe-containing CNTs	2.8% Fe	700	5000	75.1
G43-A (Ni–Pt/Al_2O_3)[13]	1–5% Ni, <1% Pt	600	6600	78.1
2800 (Raney Ni)[13]	93.8% Ni, 0.3% Fe	700	6600	81.6
146 (Ru/Al_2O_3)[13]	0.5% Ru	700	6600	84.5
Ni/MgO[14]	5% Ni	700	3600	89.2
No catalyst	—	700	5000	0.7

attribute the increased activity to the formation the nitride phase. Although iron nitride has been proposed to play a vital role in NH_3 decomposition, there is still lack of direct observation as the proof.[12] To our knowledge, this is the first study by HRTEM and EELS with element mapping to show the presence of the iron nitride phase in such catalysts, which will help future work on catalyst design and reaction mechanism.

The microstructure and chemical composition of MWCNTs were found to be unchanged after long-time exposure to NH_3 at temperatures as high as 700 °C. There is no noticeable difference in either HRTEM images or EELS of carbon nanotubes before and after reaction. X-Ray photoelectron spectroscopy (XPS) revealed that there is no observable change in the signals of both C_{1s} and N_{1s} (Fig. S3, ESI†). Therefore, the used commercial CNTs could even be utilized further. It is thus attractive to first use the metal particles in the control of the growth of CNTs and then catalyze the NH_3 decomposition to release H_2. No additional pretreatment of the CNTs is needed between these two processes.

Table 1 gives a comparison of the activities between metal-containing CNTs with various commercial decomposition catalysts taken from the literature.[13,14] Obviously, Co-containing CNTs show superior activity. Over all commercial catalysts, NH_3 conversion is lower than 90% even at a space velocity as low as 3600 ml g_{cat}^{-1} h^{-1}. The advantage of CNTs as the catalyst becomes much more evident when H_2 production rates are normalized to metal contents. The high productivities per gram of metal (mmol-H_2 g_{Metal}^{-1} min^{-1}) of Co-containing CNTs could be related to (1) the relatively small mean size of the nanoparticles (the optimal particle value is at around 2 nm, which favors high concentration of the most active B5 sites[15]) and (2) the unique capacity of CNTs as electron reservoirs, which would efficiently remove electrons from Co and promote recombinative desorption of surface nitrogen atoms as the most abundant reaction intermediate.

To summarise, we have used the commercial CNTs with residual Co- and Fe-nanoparticles as catalysts for NH_3 decomposition to produce H_2. Co-containing CNTs showed a superior activity to those reported for commercial catalysts. The microstructure of the CNTs was not damaged by NH_3 exposure at high temperature. By using microscopy with the EELS technique, we observed iron nitride as the primary active phase for NH_3 decomposition over Fe-containing CNTs.

This work was performed in the frameworks of the EnerChem of MPG and European Laboratory for Catalysis and Surface Science (ELCASS). Help from Dr Jens-Oliver Müller and Dr Di Wang on TEM tests are heartily acknowledged.

Notes and references

1 A. T–Rassi, *Proceedings of the 2002 U.S. DOE hydrogen program review*, NREL/CP–610–32405, 2002.
2 T. V. Choudhary, C. Sivadinarayana and D. W. Goodman, *Catal. Lett.*, 2001, **72**, 197.
3 J. Zhang, H. Y. Xu, X. L. Jin, Q. J. Ge and W. Z. Li, *Appl. Catal., A*, 2005, **290**, 87.
4 S. F. Yin, B. Q. Xu, X. P. Zhou and C. T. Au, *Appl. Catal., A*, 2004, **277**, 1.
5 J. Zhang, H. Y. Xu, Q. J. Ge and W. Z. Li, *Catal. Commun.*, 2006, **7**, 148.
6 A. M. Cassell, J. A. Raymakers, J. Kong and H. J. Dai, *J. Phys. Chem. B*, 1999, **103**, 6484.
7 C. Öncel and Y. Yürüm, *Fullerenes, Nanotubes Carbon Nanostruct.*, 2006, **14**, 17.
8 K. Hata, D. N. Futaba, K. Mizuno, T. Namai, M. Yumura and S. Iijima, *Science*, 2004, **306**, 1362.
9 M. Terrones, N. Grobert, J. Olivares, J. P. Zhang, H. Terrones, K. Kordatos, W. K. Hsu, J. P. Hare, P. D. Townsend, K. Prassides, A. K. Cheetham, H. W. Kroto and D. R. M. Walton, *Nature*, 1997, **388**, 52.
10 Z. F. Ren, Z. P. Huang, J. W. Xu, J. H. Wang, P. Bush, M. P. Siegal and P. N. Provencio, *Science*, 1998, **282**, 1105.
11 A. Yu, E. Bekyarova, M. E. Itkis, D. Fakhrutdinov, R. Webster and R. C. Haddon, *J. Am. Chem. Soc.*, 2006, **128**, 9902.
12 Y. Ohtsuka, C. B. Xu, D. P. Kong and N. Tsubouchi, *Fuel*, 2004, **83**, 685.
13 A. S. Chellappa, C. M. Fischer and W. J. Thomson, *Appl. Catal., A*, 2002, **227**, 231.
14 C. H. Liang, W. Z. Li, Z. B. Wei, Q. Xin and C. Li, *Ind. Eng. Chem. Res.*, 2000, **39**, 3694.
15 J. Zhang, H. Y. Xu and W. Z. Li, *Appl. Catal., A*, 2005, **296**, 257.

